

Optical Through-Focus Technique that Differentiates Small Changes in Line Width, Line Height and Sidewall Angle for CD, Overlay, and Defect Metrology Applications

Ravikiran Attota*, Richard Silver, and Bryan M. Barnes[†]

National Institute of Standards and Technology**,
Gaithersburg, MD 20899, USA

[†]KT Consulting Inc, Antioch, CA, USA

ABSTRACT

We present a new optical technique for dimensional analysis of sub 100 nm sized targets by analyzing through-focus images obtained using a conventional bright-field optical microscope. We present a method to create through-focus image maps (TFIM) using optical images, which we believe unique for a given target. Based on this we present a library matching method that enables us to determine all the dimensions of an unknown target. Differential TFIMs of two targets are distinctive for different dimensional differences and enable us to uniquely identify the dimension that is different between them. We present several supporting examples using optical simulations and experimental results. This method is expected to be applicable to a wide variety of targets and geometries.

Keywords: Through-focus image map, Optical CD (OCD) metrology, Overlay, Defect analysis, Library matching, Optical microscope, Optical inspection, Process control

1. INTRODUCTION

Semiconductor metrology faces increasing challenges with decreasing dimensions of future technology nodes. Metrology tool manufacturers are racing to overcome these challenges, often with great success. The oldest and the least expensive metrology tools are based on optics, and tremendous improvements have been made to improve optics-based metrology tools. However, optical techniques face challenges for the measurement of these ever-decreasing dimensions. Scatterometry [1] is non-imaging optical technology that has been used in semiconductor metrology with recent great success. However, its limitations are the requirement of a large target size and a repetitive structure. Alternative tools such as scanning electron microscopes (SEM) and atomic force microscopes (AFM) have also been widely used for semiconductor metrology. Although, they have the ability to analyze extremely small targets, AFMs, for example, are not conducive to the throughput demands for manufacturing. Optics-based metrology tools will continue to be used as long as they satisfy increasingly stringent measurement tolerances. Improvements in optics-based metrology tools are highly desirable due to their high throughput and low cost of ownership. In this paper, we present a new technique that extends the capabilities of optics-based imaging metrology.

In conventional optical microscopy, it is usually deemed necessary to acquire images at the "best focus" position for meaningful analysis. This is based on the belief that the most faithful representation of the target is rendered only at the best focus image. Out-of-focus images are ordinarily considered not particularly useful, especially for metrology applications. During that period in which the wavelength of the light used was much smaller than the size of the critical dimension of the semiconductor target, these assumptions were quite valid. However, the out-of-focus images do contain useful information regarding the target being imaged. The complete set of out-of-focus images contain additional information about the target as compared to a single best-focus image. This information may be obtained given an appropriate data acquisition and analysis method.

* corresponding author: ravikiran.attota@nist.gov, ** US Government work. Not subject to copyright, SPIE Vol. 6922, 2008

In previous work we proposed a new method, defined as the “focus metric signature” (FM signature) to analyze through-focus optical images for dimensional analysis [2-6]. That method utilizes a set of through-focus optical images obtained by a conventional bright-field microscope for line width analysis. Independent investigators have successfully applied the same through-focus methodology for semiconductor metrology applications [7-9]. However, similar to the scatterometry method, the FM signature method requires a repeating structure.

In this paper we present a new method of analyzing through-focus optical images for sub-100 nm dimensional metrology applications. We define this method as the “through focus image map” (TFIM) method.

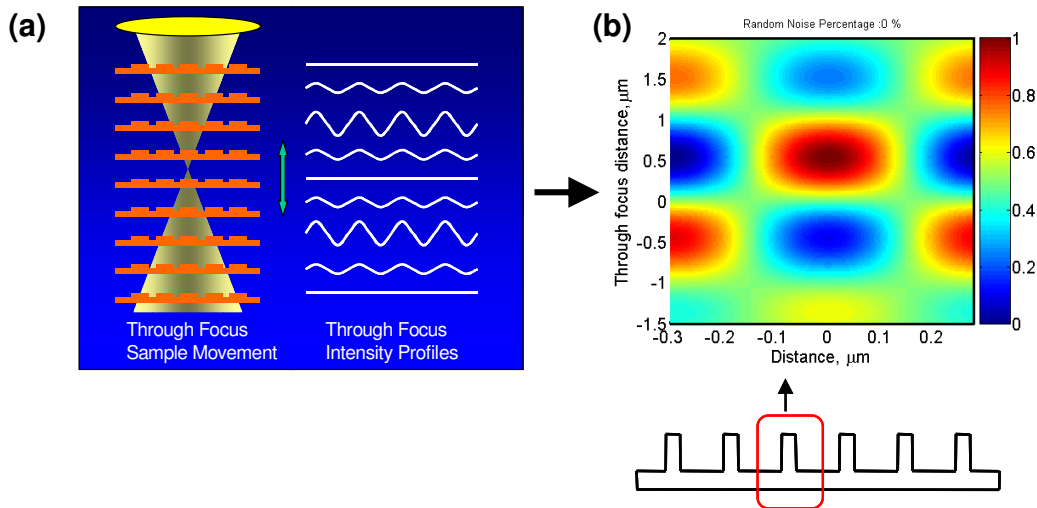


Figure 1. The method to construct the through focus image maps. (a) Schematic showing movement of a grating target and the resultant intensity profiles at different through-focus positions. (b) The simulated through-focus image map generated for the line grating under the following conditions: Line width = 152 nm, Line height = 230 nm, Pitch = 600 nm, Illumination NA = 0.36, Collection NA = 0.8, Illumination wavelength = 546 nm, Si line on Si substrate.

2. THE THROUGH FOCUS IMAGE MAP METHOD

In Fig. 1 we depict the method used for constructing the TFIM. The TFIM method uses information from out-of-focus images to enhance our image-based analysis. Simulated optical images are used here to demonstrate the method. Optical images from a target of interest (in this case, a line grating) are obtained at different focus positions (through-focus). For a two-dimensional target such as the line grating, each image at a given focus position can be reduced to an intensity profile. As the target is moved through the focus of the microscope, each focus position results in a different intensity profile, as shown in Fig. 1(a). Here, the x-axis represents the position on the target and the y-axis represents the optical intensity (the right side of Fig.1(a)). The same through-focus intensity profiles can be combined and plotted such that the x-axis represents the position on the target, the y-axis represents the focus position and the z-axis represents the optical intensity. The resultant simulated TFIM is shown in Fig. 1(b) for one cycle of an infinite line grating.

TFIMs vary substantially for different types of targets. This variation is illustrated in Fig. 2 for four types of targets. Simulations of a reflection-based optical microscope measuring an isolated line at $\lambda = 546$ nm yields the TFIM as shown in Fig. 2(a). A finite dense array with 9 lines at $\lambda = 193$ nm produces the TFIM as shown in Fig. 2 (b). This target has a pitch of 105 nm. In-chip overlay targets must be small so that they can be placed in the active area. The TFIM for an in-chip target at $\lambda = 193$ nm is shown in Fig. 2(c). TFIM may also be produced for transmission microscopy; a photo mask target in a transmission mode microscope at $\lambda = 365$ nm is shown in Fig. 2(d). This target has a chrome line on a quartz substrate.

To validate the simulation data, we collected experimental data to produce a measured TFIM. For this experiment we chose a Si line grating as the target and acquired through-focus images in our optical microscope at $\lambda = 546$ nm using a 0.36 illumination numerical aperture (NA), 0.8 collection NA, and 100 nm through-focus step increments. Using reference metrology tools such as scanning electron microscopy (SEM) and atomic force microscopy (AFM) we measured the target bottom line width as 152 nm, the line height as 230 nm and the pitch as 601 nm. Using these as input parameters to the model, we then obtained the simulated TFIM. The experimental and the simulated TFIMs are presented in Fig. 3. Good agreement between the experiment and the simulation is observed and gives us confidence in the validity of the through-focus image maps. In the next section we present applications of the TFIM for dimensional metrology.

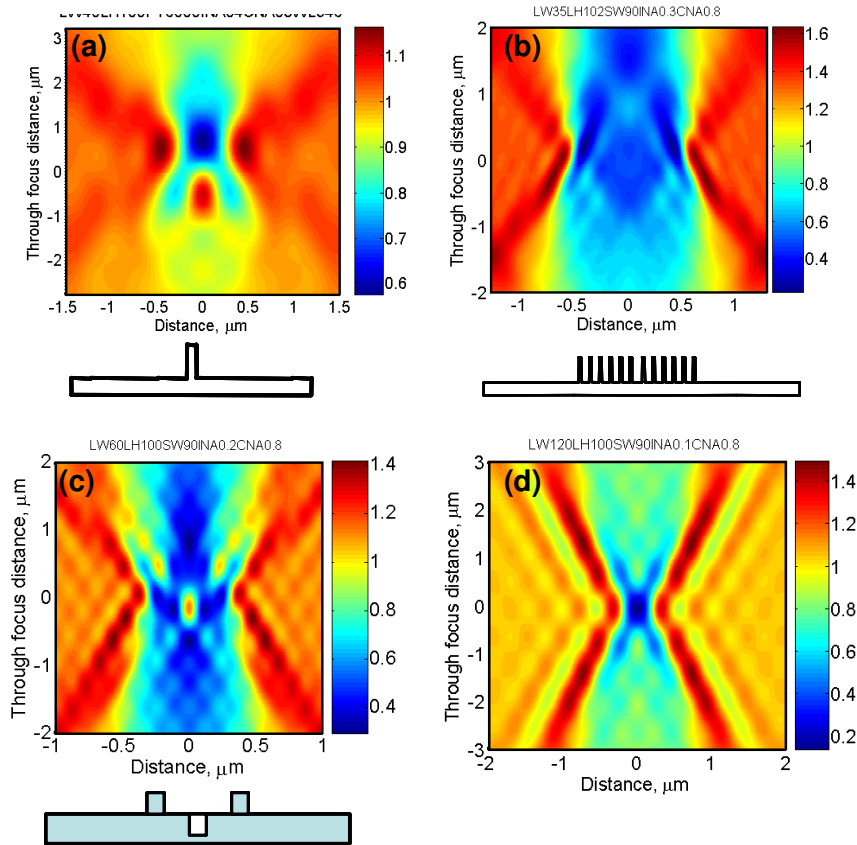


Figure 2. The simulated TFIMs for (a) an isolated Si line on a Si substrate (Line width = 40 nm, Line height = 100 nm, Illumination NA = 0.4, Collection NA = 0.8, and Illumination wavelength = 546 nm), (b) a finite dense Si array on a Si substrate (Number of lines = 9, Line width = 35 nm, Line height = 100 nm, Illumination NA = 0.3, Collection NA = 0.8, and Illumination wavelength = 193 nm), (c) an in-chip Si line on a Si substrate overlay target (Line width = 60 nm, Line height = 100 nm, Trench width = 60 nm, Trench depth = 100 nm, Distance between the lines = 400 nm, Illumination NA = 0.2, Collection NA = 0.8, and Illumination wavelength = 193 nm), and (d) a chrome line on a quartz substrate photo mask in transmission microscope mode (Line width = 120 nm, Line height = 100 nm, Illumination NA = 0.1, Collection NA = 0.8, Illumination wavelength = 365 nm).

3. TWO TYPES OF APPLICATIONS

At present we propose two broad types of applications of these TFIMs. They are:

- (i) To determine a change in the relative dimension, and
- (ii) To determine the dimensions of a target.

The first type of application, sensitivity to dimensional change, requires a minimum of two targets. As a sensitivity measurement, although simulations are not necessary, simulations greatly enhance the rigor of the method. The second type of application, determining physical dimensions, requires accurate simulations. In addition, it also requires satisfactory experiment-to-simulation agreement for successful implementation. In the current work we have used two types of optical simulation programs: rigorous coupled waveguide analysis (RCWA) [10] and finite difference time domain (FDTD) [11] programs. In the following sections we discuss these two applications of TFIMs in detail.

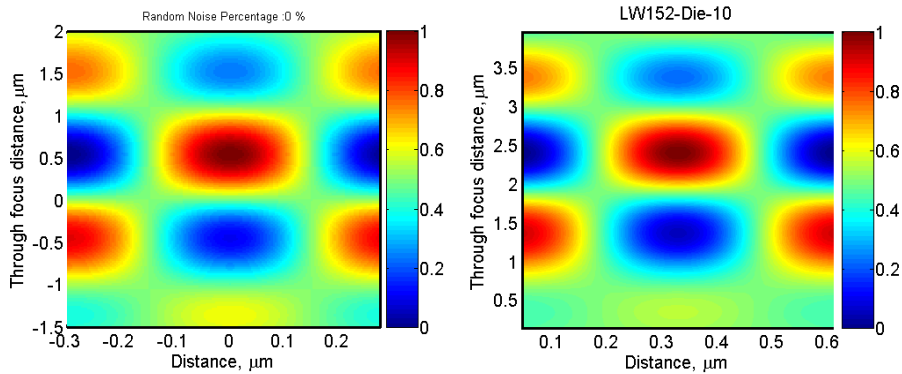


Figure 3. Comparison of (a) the simulation, and (b) the experimental TFIMs for a line grating. Line width = 152 nm, Line height = 230 nm, Pitch = 601 nm, Illumination NA = 0.36, Collection NA = 0.8, Illumination wavelength = 546 nm, Si line on Si substrate.

3.1 To determine a change in the relative dimension

A small change in the dimension of a target produces a corresponding change in the TFIM. Comparing two TFIMs from different targets, one can identify that a change in the target dimension has occurred. Although one can compare and identify changes in many ways, here we present a method based on image map differences.

Although this method can be applied to any of the targets discussed in this paper, in the current analysis we demonstrate the approach for an isolated line (*i.e.*, a line several wavelengths away from nearby features), as this is one of the more difficult targets to analyze accurately. TFIMs were simulated for small changes in the target dimensions. In Fig. 4 we present the TFIMs for two targets with 1.0 nm difference in the line width. Visual inspection of the two TFIMs would indicate that they are similar. In the same way, the TFIMs for a small change in the line height or sidewall angle also

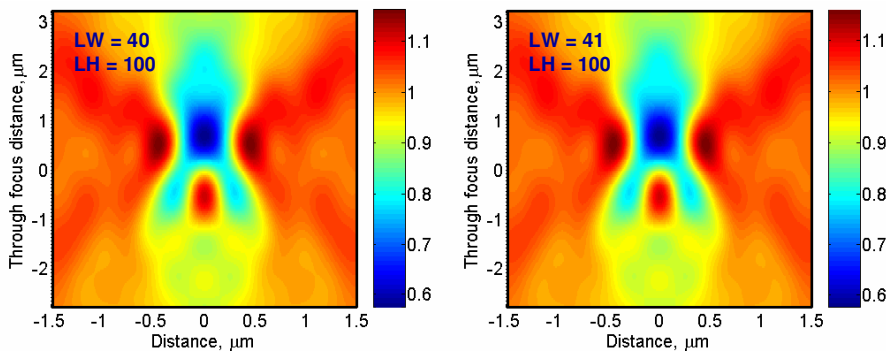


Figure 4. The simulated TFIMs two isolated line targets. LW = Line width in nm, LH = Line height in nm, Illumination NA = 0.4, Collection NA = 0.8, Illumination wavelength = 546 nm, Si line on Si substrate.

appear similar. However, a simple subtraction of any two TFIMs highlights the difference between them. This difference may be illustrated using a *differential* through-focus imaging map (DTFIM). The DTFIM is essentially the difference in the optical intensities between any two TFIMs. We analyzed the DTFIMs for four different dimensional

changes. They are a one nanometer change in the line height, a one nanometer change in the line width a one nanometer change in the line width and the line height, and a one-degree change in the sidewall angle. The DTFIMs for the four types of dimensional changes are shown in Fig. 5.

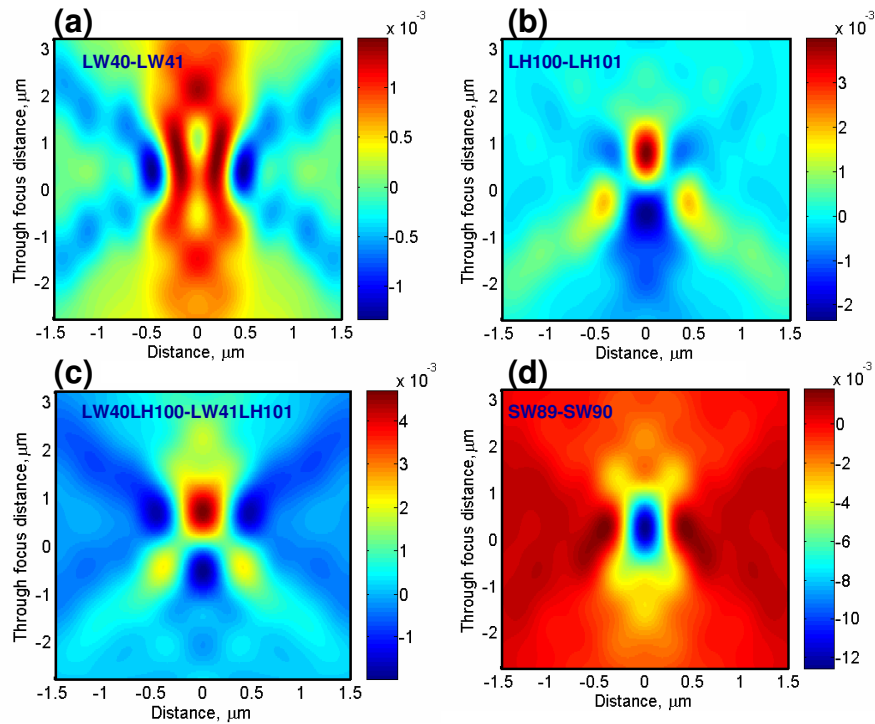


Figure 5. The simulated differential TFIMs obtained for the isolated lines shown in Fig. 4. (a) 1.0 nm change in the line width (b) 1.0 nm change in the line height (c) 1.0 nm change in the line height and the line width, and (d) one degree change in the sidewall angle.

The following observations can be made from the DTFIMs. For the simulations shown, it is possible to identify a small change in the dimension of the target using this method. However, sensitivity to small dimensional changes will depend on the measurement noise, sensitivity, and monotonic response; these are items that have not yet been investigated in depth. In the data it can be observed that a small change in the line height, the line width, both the line width and the line height, or the sidewall angle individually shows qualitatively distinct DTFIM response. We have confirmed similar simulation-based results for several different types of targets. In Figure 6 we present a second example for a finite dense line array at $\lambda = 193$ nm. Again we observe that the line height and the line width differences individually produce distinctive DTFIMs. This simulation-based analysis demonstrates an intriguing possibility for identifying specific dimensions that have changed through the examination of DTFIMs.

Next, to validate how the simulation results compare to experiment we compare an experimental DTFIM, which includes noise and other experimental imperfections, to the simulation analysis. We chose two line gratings with 146 nm and 149 nm line widths (about 3 nm difference). Using $\lambda = 546$ nm light, we obtained two experimental TFIMs to yield one DTFIM. The process of obtaining the experimental DTFIM requires some explanation; we normalized intensities of the experimental TFIMs such that the maximum intensity in the image equals to one and the minimum intensity equals to zero. The two normalized TFIMs were then aligned such that the maximum intensity peaks coincided. At this point DTFIMs were obtained. We applied the same normalization procedure to the simulation results to maintain consistency with the experiment. The DTFIMs from the simulations and the experiments are shown in Fig. 7. Although agreement is far from ideal, the experimental and simulated DTFIMs have substantial qualitative similarities. The experimental data was obtained using an optical microscope that had not been characterized with the recently discovered techniques as

presented in Ref. [12]. It is our belief that characterizing the microscope with the improved techniques would substantially enhance the experimental agreement with the simulations.

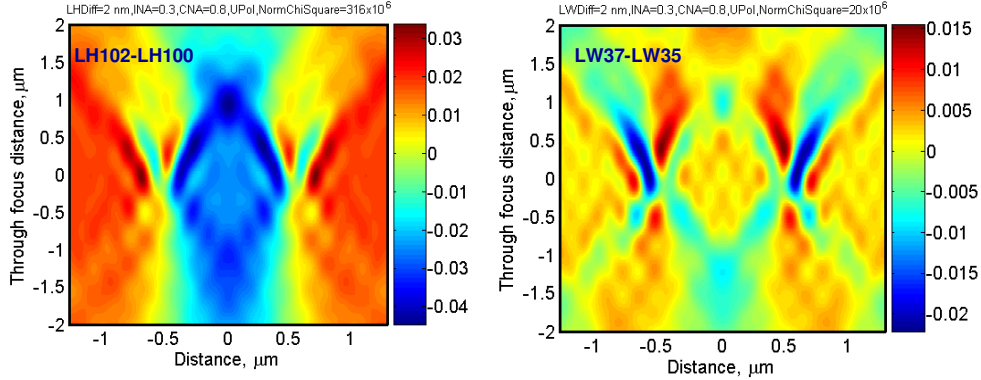


Figure 6. The simulated DTFIM obtained for finite dense arrays for (a) 2.0 nm change in the line height, and (b) 2.0 nm change in the line width. Line width = 35 nm, Line height = 100 nm, Illumination NA = 0.3, Collection NA = 0.8, Illumination wavelength = 546 nm, Si line on Si substrate.

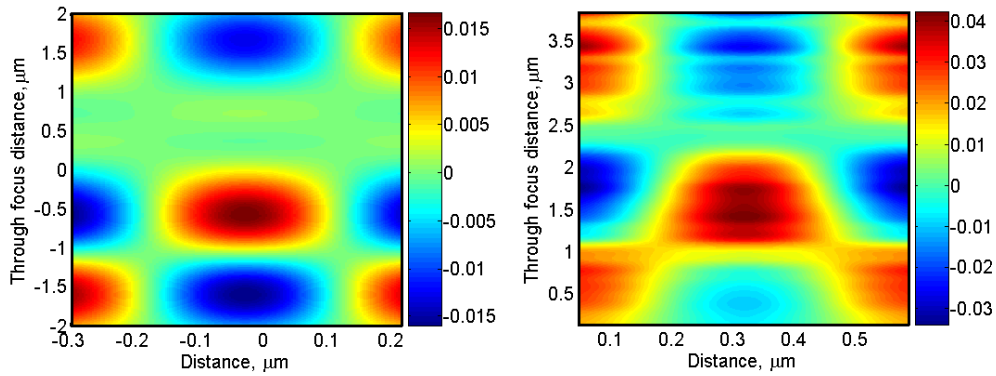


Figure 7. Comparison of (a) the simulation and (b) the experimental differential images. The differential images were obtained for the two targets with line widths of 146 nm and 149 nm. Line height = 230 nm, Pitch = 601 nm, Illumination NA = 0.36, Collection NA = 0.8, Illumination wavelength = 546 nm, Si line on Si substrate.

As shown above, different dimensional changes (i.e width or height) produce qualitatively distinct DTFIMs. However, for different magnitude changes of the same dimension, qualitatively the DTFIMs appear similar. In Figs. 8(a) and (b) we present the DTFIMs for 1.0 nm and 2.0 nm differences in the line width, respectively, for an isolated line at $\lambda = 546$ nm. Similarly, we present the DTFIMs for 1.0 nm and 4.0 nm differences in the line heights in Figs. 9(a) and (b), respectively, for an isolated line for $\lambda = 193$ nm. These simulations yield qualitatively similar appearing DTFIMs. We performed a similar analysis for several different types of targets under different conditions. In all the cases tested we observed a similar behavior. This behavior holds true as long as the difference in the dimensional magnitude is small compared to the dimension. It is also important to note that the differences in the DTFIMs for different types of dimensional changes are much stronger compared to differences in the DTFIMs for different magnitudes of the same dimensional changes.

To quantify the magnitude of the difference for a single parameter, we evaluate the “Sum Difference Square” (SDS), which is defined here as :

$$\text{Sum Difference Square} = \Sigma (\text{TFIM}_1 - \text{TFIM}_2)^2$$

Since the SDS value depends on the density of the points in the image, we normalize the SDS by dividing it by the total number of points in the image. The SDS also depends on the selection of the portion of the DTFIM. In the DTFIM shown in Fig. 10, selecting the larger outer area results in a smaller SDS value. Whereas selecting the smaller portion as indicated by the smaller inner box results in a relatively larger SDS value. For comparing different results we kept the selected area the same.

We evaluated the SDS values for the DTFIMs presented in Figs. 8 and 9. For 1.0 nm and 2.0 nm differences in the line widths (Fig. 8) we get SDS values of 6.0×10^{-8} and 2.05×10^{-8} respectively. Similarly, 1.0 nm and 4.0 nm differences in the line heights (Fig. 9) produce SDS values of 0.72×10^{-6} and 3.0×10^{-6} respectively. This demonstrates that the SDS value increases with the magnitude of the difference of a given dimension. However, the amount of increase depends on the individual case.

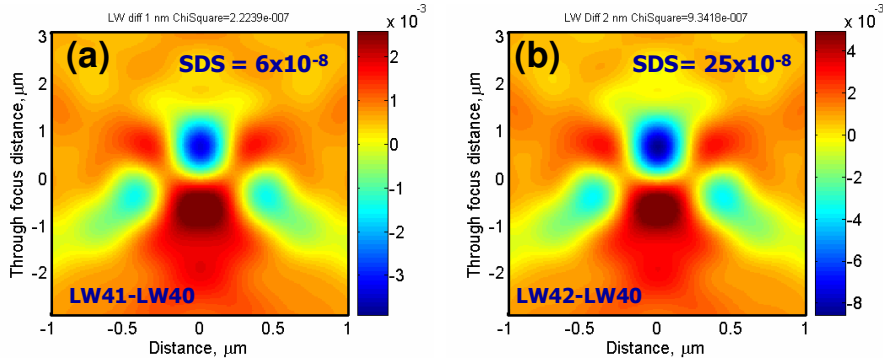


Figure 8. The simulated DTFIM obtained for (a) the line widths of 41 nm and 40 nm (1.0 nm difference), and (b) the line widths of 42 nm and 40 nm (2.0 nm difference). Isolated line, Line height = 100 nm, Illumination NA = 0.4, Collection NA = 0.8, Illumination wavelength = 546 nm, Si line on Si substrate.

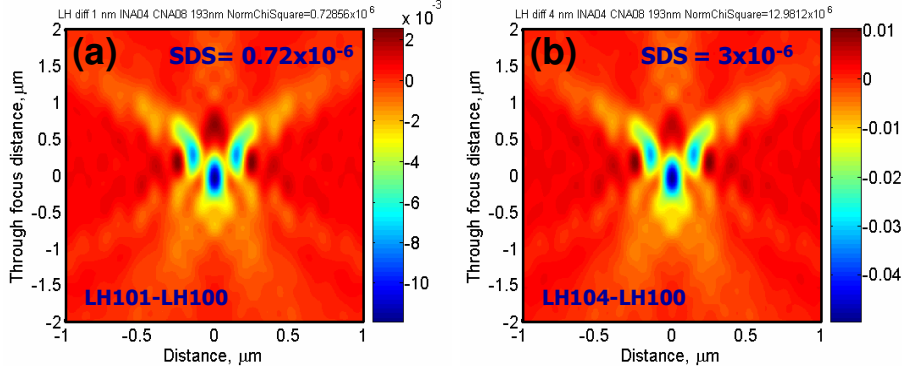


Figure 9. The simulated DTFIM obtained for (a) line heights 101 nm and 100 nm (1.0 nm difference), and (b) line heights 104 nm and 100 nm (4.0 nm difference). Isolated line, Line width = 40 nm, Illumination NA = 0.4, Collection NA = 0.8, Illumination wavelength = 193 nm, Si line on Si substrate.

The polarization state of the illumination produces different sensitivities for a given dimensional difference. This is illustrated in Fig. 11 for an isolated line at $\lambda = 193$ nm and 100 nm nominal line height for un-polarized, TE-polarized (electric field pointing along the lines), and TM-polarized (electric field pointing perpendicular to the lines) illuminations. This figure shows that the TFIMs and the DTFIMs are strong functions of the illumination polarization. More importantly, we see a large difference in the SDS value depending on the illumination polarization for a 2.0 nm difference in the line height. Under the present simulation conditions, TM polarization produces the maximum sensitivity for a given line height difference. In a similar way, for any given experimental conditions, one can choose the illumination polarization that gives the maximum sensitivity for a given dimensional difference.

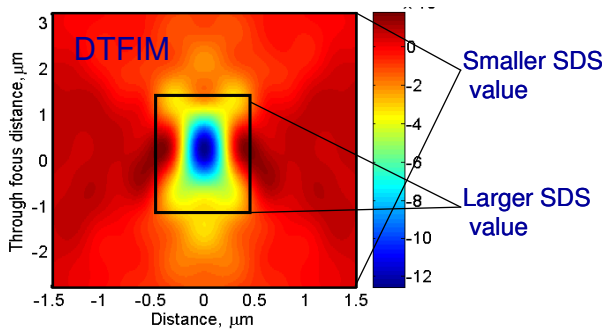


Figure 10. Illustration showing the dependence of the SDS value on selection of the portion of the DTFIM.

Using simulations, one can optimize the experimental conditions to produce a maximum sensitivity. We chose a photomask target for a transmission microscope to demonstrate this optimization method. The photomask target has an isolated chrome line on a quartz substrate. The line width and the line height of the chrome line are 120 nm and 100 nm respectively. We optimize sensitivity as determined by the SDS value for a 2.0 nm difference in the line width and the line height as a function of the polarization and the illumination NA as shown in Fig. 12. Under the given simulation conditions, a low 0.1 illumination NA produces a high sensitivity, both for the line width and the height variations. However, the line width exhibits the highest sensitivity for TE illumination polarization, whereas the line height shows the highest sensitivity for TM illumination polarization.

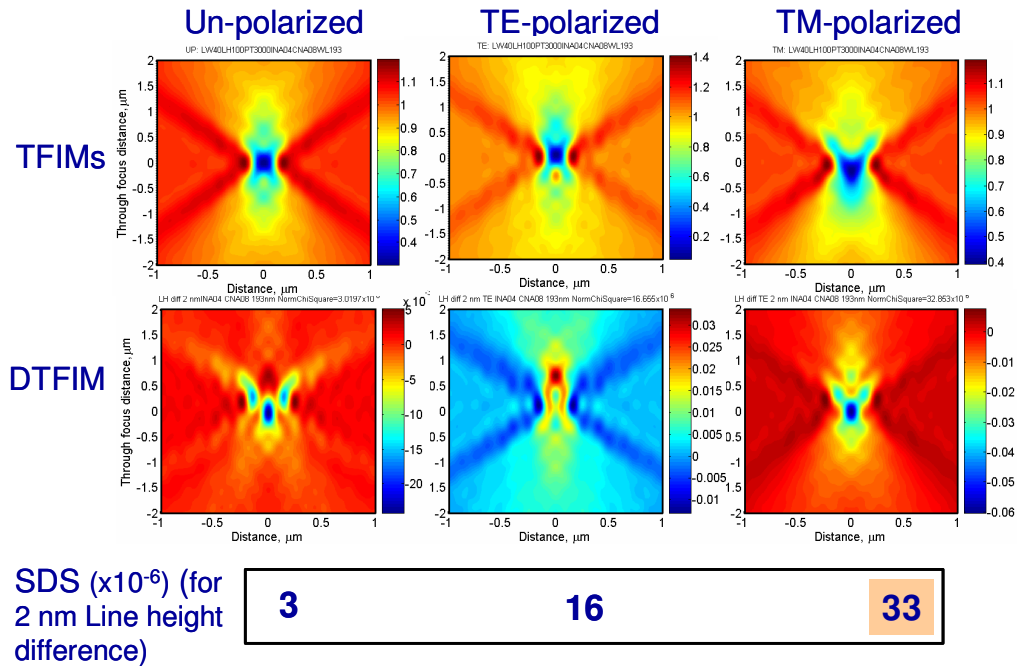


Figure 11. Effect of polarization on the TFIMs, the differential images and the SDS values. Isolated line, Line width = 40 nm, Line height = 100 nm, Illumination NA = 0.4, Collection NA = 0.8, Illumination wavelength = 193 nm, Si line on Si substrate.

Two simulation results at $\lambda = 193$ nm illumination wavelength demonstrate target-specific overlay applications. Our first target is a finite dense array with 9 lines as shown in Fig. 13(a). We present analysis for an overlay offset of 2.0 nm of each alternate line as shown in Fig. 13(a). The DTFIM obtained using the base target (zero overlay offset) and the target with 2.0 nm offset is shown in Fig. 13(b). The DTFIM shows good signal strength and sensitivity for a 2.0 nm overlay. A line is drawn in the DTFIM to indicate the center of the target. Positive or negative overlay values may be identified by analyzing the symmetry of the DTFIM about this center line. This type of target analysis has applications in double patterning.

In Fig. 14(a) we present a second overlay target, which is an in-chip target. These types of targets are designed to be placed in the active area of the chip because of their extremely small footprint. The in-chip target has two projecting lines and a trench line between them. The distance between the two projecting lines is 400 nm. We studied overlay offsets of the center line ranging from -6.0 nm to +6.0 nm using TE and TM illumination polarizations. The other relevant simulation conditions for this target are given in Fig. 14. A typical DTFIM between the base target (with zero overlay), and the target with 6.0 nm positive overlay is shown in Fig. 14(b) for TM polarization. It produces a very high SDS value of 218. We evaluated the SDS values for the different overlay offsets and obtained the overlay-calibration curve as shown in Fig. 14(c). TM polarization shows higher sensitivity to overlay under the current simulation conditions. Once we obtain the calibration curve, the experimental SDS values can be compared to it to determine the overlay offset. In fact, one can generate a similar calibration curve and follow the same procedure to determine the overlay offset for the finite dense array shown in Fig. 13.

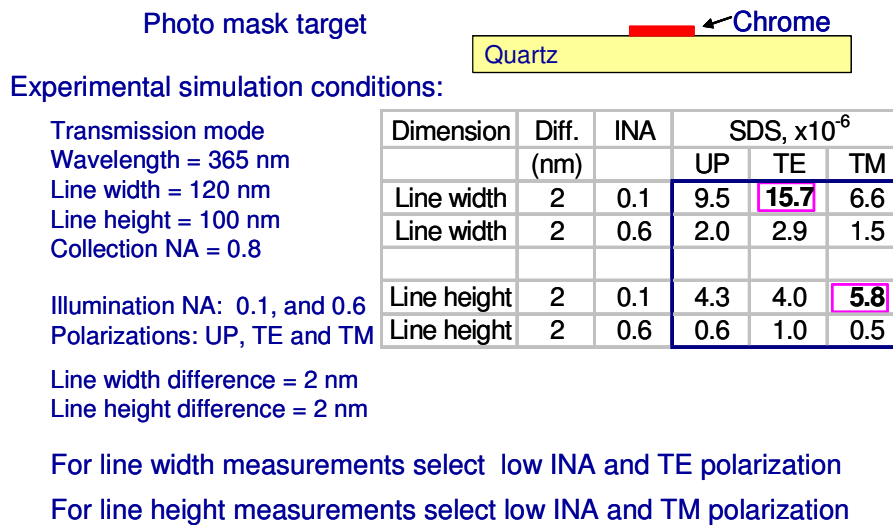


Figure 12. Method to optimize the measurement sensitivity (maximize the SDS value) for a photo mask target in transmission microscope mode.

3.2 Analysis to Determine the Dimension of the Target

The utility of the TFIM approach in metrology is based on an assumption that any given target produces a unique TFIM. This assumption was satisfactorily tested for two particular cases: an isolated line and a line grating targets using simulations. Additional analysis will require the simulation of a library of TFIMs for all the possible combinations of the target dimensions for a set of given experimental conditions. The experimental TFIM can then be compared with the database. The simulated TFIM from the library which best matches the experimental TFIM would yield the dimension of the target.

First we present a uniqueness test using the simulations for a line grating. For this we simulated a small library of the TFIMs for line widths varying from 145 nm to 155 nm and line heights varying from 125 nm to 135 nm. We used a 1.0 nm step increment for both the line width and the line height to produce a total of 121 simulation combinations. We then generated another set of 'unknown' target simulations, the dimensions of which do not exactly match that of the targets in the library as shown in the table in Fig. 15. These 'unknown' targets were then compared to the library by evaluating their SDS values. A plot of the SDS values thus obtained is shown in Fig. 15 for the line width of 146.2 nm and the line height of 233.8 nm. The minimum SDS value gives the best matched target. The best matched targets for the three 'unknown' targets are presented in the Table in Fig. 15. The agreement is satisfactory.

We then applied the same technique to measure experimentally the line width of the line grating target shown in Fig. 3(b). Since this is the first application of this technique to measure the line width experimentally the results are

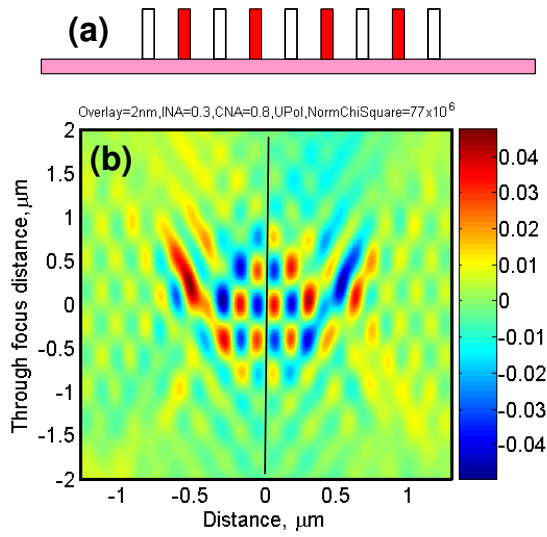


Figure 13. Overlay application of the differential image for a finite dense array. (a) The target showing the filled lines that move relative to the unfilled lines with the given overlay offset, and (b) The differential image for a 2.0 nm overlay with the central line showing the axis of symmetry. Line width = 35 nm, Line height = 100 nm, Pitch = 105 nm, Illumination NA = 0.3, Collection NA = 0.8, Illumination wavelength = 193 nm, Si line on Si substrate.

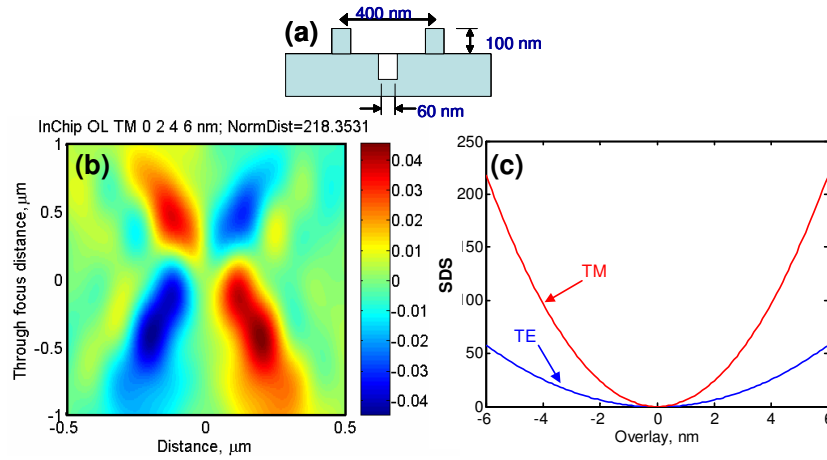


Figure 14. Application of the differential image for an in-chip overlay target. (a) The target showing the dimensions of the in-chip target, (b) The differential image for a 6.0 nm overlay, and (c) The overlay calibration curve generated using the Chi Square values for TE and TM polarizations. Illumination NA = 0.2, Collection NA = 0.8, Illumination wavelength = 193 nm, Si line on Si substrate.

4. SUMMARY

This paper presents a novel technique to use the additional information contained in a set of through-focus optical images as compared to one image at the best focus position. Two-dimensional through-focus image maps (TFIM) were presented to analyze dimensional information of sub 100 nm targets. The TFIMs are formed by stacking the through-focus optical image intensity profiles such that the X-axis represents the lateral distance on the target, the Y-axis represents the through focus position and the intensity of the image (the Z-axis) represents the optical intensity. We

preliminary in nature. We determined all the dimensions of the selected target, including the line width, using reference metrology tools such as scanning electron microscope (SEM) and atomic force microscope (AFM). The SEM measured line width was 152 nm for the selected target. However, we assumed the line width to be ‘unknown’. Using the measured dimensions we simulated a small library of TFIMs by keeping the line height (230 nm), the pitch (601 nm), and the sidewall angle (which is curved) constant. For the simulation of the library, we varied only the line width from 144 nm to 156 nm with a step increment of 0.5 nm. The library matching of the experimental TFIM (Fig. 3(b)) was carried out by evaluating the SDS values from the DTFIM. The DTFIM between the experimental and the simulated TFIM was obtained after they were aligned to get the best match. A plot of the SDS values thus evaluated as a function of the line width in the library is shown in Fig. 16. The inset shows the magnified view of the bottom of the curve. This gives the best line width match as 153 nm, which is close to the SEM measured line width of 152 nm. Even though the TFIM based line width matches very close to the SEM measured line width, its value differs substantially with the AFM measured line width of 140 nm. The discrepancy among the SEM, the AFM and the optical technique used here requires further study and is beyond the scope of the current paper.

proposed two main applications of the TFIMs: (i) to determine a change in the relative dimension and (ii) to determine the dimensions of a target. We presented several examples using the optical simulations and the experimental results.

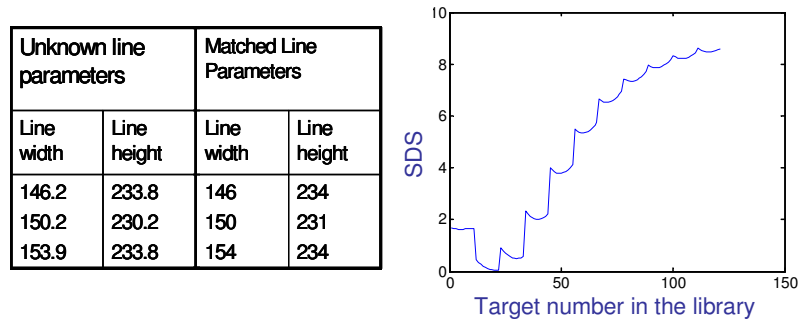


Figure 15. Demonstration of the uniqueness test using the simulations. (a) The table showing the unknown line parameters and the matched line parameters from the library. All the dimensions are in nanometers. (b) A typical plot of SDS values evaluated using the library for the unknown target with line width of 146.2 nm and line height of 233.8 nm.

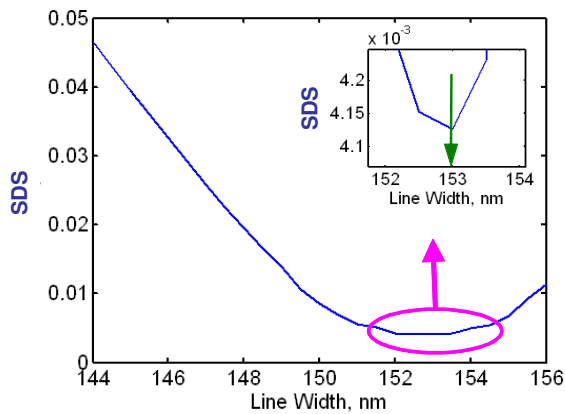


Figure 16. A plot of the SDS values evaluated using the experimental 'unknown' target with the library of simulations. The inset shows the magnified portion of the highlighted curve.

DTFIMs of the TFIMs are distinctive for different parametric changes. They enable us to identify which parameter is different between two targets. However, the DTFIMs obtained for different magnitude changes of the same parameter appear qualitatively similar. In this case, the SDS value, which is defined here as $\Sigma (\text{DTFIM})^2$, enables us to determine the magnitude of the difference in the dimension. The TFIM enables us to determine the dimensions of an unknown target by the library matching method, provided we have the accurate simulations and the experimental results for a fully characterized optical microscope. We expect this method to be applicable to a wide variety of targets with a variety of applications including, but not limited to critical dimension (CD) metrology, overlay metrology, defect analysis and process control. Future work includes extending the current method to three-dimensional targets.

5. ACKNOWLEDGEMENTS

The authors would like to thank Jim Potzick for the useful discussions. The NIST Office of Microelectronics Programs is gratefully acknowledged for financial support as well as the NIST Scatterfield Competence project. The authors thank Sematech for wafer fabrication and measurement support.

6. REFERENCES

1. C.J. Raymond, S.S.H. Naqvi, and J.R. McNeil, "Scatterometry for CD measurements of etched structures," Proc. SPIE, **2725**, p. 720-728 (1996).
2. R. Attota, R. M. Silver, M. Bishop, E. Marx, J. Jun, M. Stocker, M. Davidson, and R. Larrabee, "Evaluation of New In-chip and Arrayed Line Overlay Target Designs," Proc. SPIE, **5375**, p. 395-402 (2004).
3. R. M. Silver, R. Attota, M. Stocker, M. Bishop, J. Jun, E. Marx, M. Davidson, and R. Larrabee, "High resolution optical overlay metrology," Proc. SPIE, **5375**, p. 78-95 (2004).

4. R. Attota, R. M. Silver, T. A. Germer, M. Bishop, R. Larrabee, M. T. Stocker, L. Howard, "Application of Through-focus Focus-metric Analysis in High Resolution Optical Metrology" Proc. SPIE, **5752**, p. 1441-1449 (2005).
5. Ravikiran Attota, Richard M. Silver, and James Potzick, "Optical illumination and critical dimension analysis using the through-focus focus metric," Proc. SPIE, **6289**, p. 62890Q-1-10 (2006).
6. Ravikiran Attota, Richard M. Silver, and Ronald Dixson, "Line width measurement technique using through-focus optical images," Applied Optics, **47**, p. 495-503, (2008).
7. Yi-Sha ku, An-Shun Liu, and Nigel Smith, "Through-focus technique for nano-scale grating pitch and linewidth analysis," Optics Express, **13**, p. 6699-6708 (2005).
8. An-Shun Liu, Yi-Sha ku, and Nigel Smith, "Through-focus algorithm to improve overlay tool performance," Proc. SPIE, **5908**, 383-391 (2005).
9. Yi-Sha ku, An-Shun Liu, and Nigel Smith, "Through-focus technique for grating linewidth analysis with nanometer sensitivity," Optical Engineering, **45**, 123602-1-6 (2006).
10. M. Davidson, "Analytic waveguide solutions and the coherence probe microscope," Microelectronic Engineering, **13**, p. 523-526 (1991).
11. T.V. Pistor, "Electromagnetic Simulation and Modeling with Applications in Lithography", Ph.D. Thesis, Memorandum No. UCB/ERL M01/19, May 1, 2001.
12. R. M. Silver, B.M. Barnes, Alan Heckert, R. Attota, T. Germer and J. Jun, "Angle resolved optical metrology," Presented at Advanced Microlithography, San Jose, CA, (2008).

**Presented at SPIE Advanced Lithography: Metrology Inspection and Process Control for
Microlithography XXII, Vol. 6922, San Jose, CA, USA, 24-29 February 2008**